UNIVERSIDADE DE SÃO PAULO

INSTITUTO DE FÍSICA
CAIXA POSTAL 20516
01000 - SÃO PAULO - SP
BRASIL

IFUSP/P 341
B.I.F. - USP

publicações

IFUSP/P-341

THE ELECTRODISINTEGRATION OF ^{63}Cu AND ^{65}Cu

by

M.N. Martins, E. Wolynec and M.C.A. Campos

Instituto de Física, Universidade de São Paulo,
São Paulo, S.P., Brazil

B.I.F. - USP

Julho/1982

The Electrodisintegration of ^{63}Cu and ^{65}Cu

M.N. Martins, E. Wolynec and M.C.A. Campos

Instituto de Física da Universidade de São Paulo
São Paulo, S.P., Brazil

Abstract

The (e,α) cross section for ^{65}Cu has been measured in the electron energy range 14-34 MeV. The results have been analyzed using the distorted-wave Born approximation E1 and E2 virtual photon spectra and the E1 and E2 components of the corresponding (γ,α) cross section were obtained. To assess the accuracy of the virtual photon analysis, the $(e,2n)$ cross section for ^{63}Cu was also measured and the obtained $(\gamma,2n)$ cross section is compared with direct measurement of this cross section performed with annihilation gamma rays.

Nuclear Reactions $^{65}Cu(e,\alpha)$ and $^{63}Cu(e,2n)$

Measured $\sigma_{e,\alpha}(E_o)$ and $\sigma_{e,2n}(E_o)$

Deduced $\sigma^{E1}_{\gamma,\alpha}(E)$, $\sigma^{E2}_{\gamma,\alpha}(E)$ and $\sigma^{E1}_{\gamma,2n}(E)$.

PACS numbers: 25.30.Cg , 24.30.Cz , 25.20.+y

I. Introduction

The (e,α) cross section has been measured for several nuclei[1,2] and the results were analyzed using DWBA virtual photon spectra[3,4] to obtain the E1 and E2 components of the corresponding (γ,α) cross section.

In this paper we use the same technique described in refs. 1 and 2 to study the (e,α) cross section in ^{65}Cu. This technique takes advantage of the fact that the E2 virtual photon spectrum is enhanced relatively to the E1 spectrum, as shown in Fig. 1, while the bremsstrahlung spectrum contains all multipoles in equal amounts. The E1 and E2 components of the (γ,α) cross section are obtained from combined measurements of the electrodisintegration cross section and the corresponding yield of electro plus photodisintegration induced by bremsstrahlung.

The (γ,α) cross section is known for many nuclei and in almost all studied cases it has a resonant shape. However, for two nuclei, ^{90}Zr [5] and ^{65}Cu [6], the (γ,α) cross section, obtained from measurements of the (e,α) cross section, showed a non resonant behaviour. For these nuclei the (γ,α) cross section increases continuously with the photon energy up to the maximum energy studied, which was $\sim$ 60 MeV. An attempt was made to explain the strange behaviour of the (γ,α) cross section in ^{90}Zr, using a pre-equilibrium exciton model combined with the quasi-deuteron model[5].

This has motivated us to study the (e,α) cross section in ^{65}Cu, since it can easily be measured by residual activity. In ref. 6 the (e,α) cross section was measured by counting directly the alpha particles emitted at 90^{o} to the electron beam.

In order to assess the accuracy of the technique employed in the analysis we have measured the $(e,2n)$ cross section for ^{63}Cu. The choice was based in several reasons. The $(\gamma,2n)$ cross section is well known for this nucleus and it is above the isoscalar E2 and bellow the isovector E2 resonances. Thus we can be sure it is an E1 process. Eventhough there are many experimental tests of the E1 virtual photon spectra and all show excellent agreement between calculation and experiment, it has been pointed out by Ströher[7] that no conclusive tests of the E1 virtual photon spectra exists, since the investigated reaction data were analyzed with the assumption of a pure E1 excitation, in cases were E2 excitation could give a significative contribution. Furthermore, the $(e,2n)$ cross section can also be measured by radioactivity and yields the same gamma ray line used to measure the (e,α) cross section, as discussed in the next section. Consequentely, the results also test the reliability of our measurements.

II. The Experiment

The experiment was performed using the electron linear accelerator of Universidade de São Paulo. Table I gives target thicknessess and enrichments. The (e,α) and $(e,2n)$ cross sections were measured by counting the induced residual activity. For the (e,α) cross section in ^{65}Cu we measured the 67.4 keV gamma ray which follows the decay of $^{61}Co \rightarrow {}^{61}Ni + \beta^{-}$, with a half life of $(1.650 \pm 0.005)h$ [8]. For the $(e,2n)$ cross section we measured the same 67.4 keV gamma ray, since ^{61}Cu decays to

^{61}Ni with a half life of (3.41 ± 0.01)h[9]. Fig. 2 shows a typical gamma ray spectrum. It is important to notice that there are no nearby lines, which could contribute to uncertainties in deriving the cross sections. As a check of our data, we measured both half lives, after irradiating the targets with 30 MeV electrons, and the decay constants obtained are compared with values from the literature in Table II.

In order to obtain the electro plus photodisintegration yields, a 0.717 g/cm^2 copper radiator was placed in the electron beam, ahead of the target, without any spacing between the radiator and the target.

III. Results and Analysis

The electrodisintegration cross section $\sigma_{e,x}(E_o)$ may be obtained from the photonuclear cross section $\sigma^{\lambda L}_{\gamma,x}(E)$ through an integral over the virtual photon spectrum $N^{\lambda L}(E_o,E,Z)$:

$$\sigma_{e,x}(E_o) = \int_0^{E_o-m} \sum_{\lambda L} \sigma^{\lambda L}_{\gamma,x}(E) N^{\lambda L}(E_o,E,Z) \frac{dE}{E} \qquad (1)$$

In Eq. (1), E_o stands for the total electron energy and E stands for the excitation energy of multipolarity λL. In the same spirit the yield with the radiator in is:

$$Y_{e,x}(E_o) = \sigma_{e,x}(E_o-2\Delta E_o) + N_r \int_0^{E_o-m} \sum_{\lambda L} \sigma^{\lambda L}_{\gamma,x}(E) K(E_o-\Delta E_o,E,Z_r) \frac{dE}{E} \qquad (2)$$

where N_r is the number of nuclei/cm^2 in the copper radiator, $K(E_o,E,Z_r)$ is the bremsstrahlung cross section in copper, and ΔE_o is the electron energy loss in half the radiator thickness. We have used the Davies-Bethe-Maximon[10] bremsstrahlung cross section. The size correction discussed in ref. 2 was applied to the virtual photon spectra. This correction, for 35 MeV electrons, amounts to 2% for the E1 and 8% for the E2 spectra.

The measured (e,2n) and (e,α) cross sections (circles) and the corresponding yields of electro plus photodisintegration (squares) are shown in Figs. 3 and 4. In Fig. 4 the triangles show the (e,α) cross section from ref. 6. In order to compare with our results, we have multiplied their 90 degrees cross section by 4π, since previous measurements have shown that the angular distribution is nearly isotropic[11,12].

The cross sections $\sigma_{e,x}(E_o)$ and the yields $Y_{e,x}(E_o)$ have been simultaneously fitted, using Eqs. (1) and (2) with the photonuclear cross sections represented by histograms.

As discussed previously, for the (γ,2n) cross section we used only E1 multipolarity. The histogram in Fig. 5 shows the (γ,2n) cross section obtained from our measurements. The experimental points show the (γ,2n) cross section measured by Fultz et al.[13]. There is good agreement between the (γ,2n) cross section derived from our electrodisintegration measurement and the cross section measured with annihilation gamma rays. Our integrated (γ,2n) cross section, up to 27.8 MeV (maximum energy measured by ref. 13) is 79.3 ± 2.2 MeV.mb, while Fultz obtains 76 MeV.mb. The difference of 4.5% in the integrated strength is

well within the uncertainties of the absolute values of both experiments.

Fig. 6 shows the ratio of measured to calculated (e,2n) cross section (circles) and measured to calculated electro plus photodisintegration yield (triangles). This is the ratio between the measured points and the calculated full curves of Fig. 3. This figure shows the compatibility between electro and photodisintegration, that is, between the E1 virtual photon spectrum and the bremsstrahlung spectrum. These results give confidence to our measurement and the analysis employed to derive the photonuclear cross section.

Fig. 7 shows the histograms obtained for the E1 and E2 components of the (γ,α) cross section. The E1 component exhausts 0.97 ± 0.14 percent of the dipole sum and the E2 component 3.2 ± 1.2 percent of the energy weighted sum rule for isoscalar E2. The points show the (γ,α) cross section from ref. 6, multiplied by 4π. It was obtained by unfolding of the (e,α) cross section assuming a pure E1 process, but this would introduce only a small error in the derived (γ,α) cross section. The strong disagreement between our (γ,α) cross section and that from ref. 6 does not come from the analysis, but from disagreement in the experimental data. In Fig. 8 we show the ratio between the (e,α) cross section of ref. 6 and the present measurement. Their cross section is only 0.13 of our value at 15 MeV and reaches 0.79 of our value at 34 MeV.

In Table III we compare the E1 and E2 strengths in the (γ,α) cross section of ^{65}Cu with other nuclei in this mass region. The (γ,α) cross section in ^{65}Cu is smaller than for

other nuclei, but like the other nuclei studied, the E2 component exhausts a larger fraction of the E2 sum, relatively to the E1. The strength of the (γ,α) cross section shows large variations in these nuclei, being 78 MeV.mb for ^{64}Zn and only 10 MeV.mb for ^{65}Cu. However, these large differences result mostly from differences in binding energies, Coulomb barrier heights and competition with other channels, as already pointed out by Dodge et al.[2]. The (γ,α) cross section in ^{65}Cu is similar in shape and magnitude to ^{62}Ni or ^{59}Co. The dominant statistical nature of the (γ,α) cross section in the nuclei listed in Table III is evident from the spectrum of the emitted alpha particles, which is of evaporation type, peaking at the energy of the Coulomb barrier[1,2]. In the present work we did not observe the emitted alpha particles, but their spectrum is known from previous work[11,12]. It has to be pointed out that in this respect the alpha particle spectrum from ^{90}Zr[5] is also of the evaporation type, peaking at the energy of the Coulomb barrier height. Since, now, the only nucleus with a non resonant (γ,α) cross section is ^{90}Zr, the results obtained for ^{65}Cu suggest that the ^{90}Zr (e,α) cross section should be measured again before developing calculations for reaction mechanisms involving cascade processes that could account for a non resonant (γ,α) cross section[5].

IV. Conclusions

The measurement of the (e,2n) and (e+γ,2n) cross sections for ^{63}Cu tests the E1 virtual photon spectrum in a situation where E2 contributions can be ruled out. The agreement between photo

and electrodisintegration is very good. The $(\gamma,2n)$ cross section obtained from this measurement agrees well with the shape and absolute magnitude of available $(\gamma,2n)$ data.

The (e,α) cross section in ^{65}Cu is in disagreement with previous measurements in magnitude and shape. The (γ,α) cross section derived from our measurements has the expected resonant shape and fits well in the systematics of nuclei in this mass region. The E1 and E2 components of the (γ,α) cross section are both small but the E2 component is relatively more important.

Acknowledgements

The authors would like to thank Profs. Giorgio Moscati and J. Goldemberg for many useful discussions and for reading the manuscript, and Conselho Nacional de Desenvolvimento Científico e Tecnológico, Fundação de Amparo à Pesquisa do Estado de São Paulo and Financiadora de Estudos e Projetos for financial support.

References

1. E. Wolynec, W.R. Dodge, R.G. Leicht and E. Hayward, Phys. Rev. C 22, 1012 (1980).
2. W.R. Dodge, R.G. Leicht, E. Hayward and E. Wolynec, Phys. Rev. C 24, 1952 (1981).
3. W.W. Gargaro and D.S. Onley, Phys. Rev. C 4, 1032 (1971).
4. C.W. Soto Vargas, D.S. Onley and L.E. Wright, Nucl. Phys. A 288, 45 (1977).
5. T. Tamae, T. Urano, M. Hirooka and M. Sugawara, Phys. Rev. C 21, 1758 (1980).
6. T. Tanaka, Research Report of Laboratory of Nuclear Science, Tohoku University 14, 137 (1981) and private communication.
7. H. Ströher, R.D. Fisher, J. Drexler, K. Huber, U. Kneissl, R. Ratzek, H. Ries, W. Wilke and H.J. Maier, Phys. Rev. Lett. 47, 318 (1981).
8. L.A. Smith, R.N.H. Haslam and J.G.V. Taylor, Phys. Rev. 84, 842 (1951).
9. J.C. Ritter and R.E. Larson, Nucl. Phys. A127, 399 (1969).
10. J.L. Mathews and R.O. Owens, Nucl. Instrum. Methods 111, 157 (1973).
11. J.J. Murphy II, H.J. Gehrhardt and D.M. Skopik, Nucl. Phys. A277, 69 (1977).
12. J.J. Murphy II, D.M. Skopik, J. Asai and J. Uegaki, Phys. Rev. C18, 736 (1978).
13. S.C. Fultz, R.L. Blamblett, J.F. Caldwell and R.R. Harvey, Phys. Rev. B133, 1149 (1964).

Figure Captions

Figure 1 El and E2 virtual photon spectra for 30 MeV electrons inelastically scattered from a copper nucleus.

Figure 2 Typical gamma ray spectrum observed in the decay of ^{61}Co , obtained from the reaction $^{65}Cu(e,\alpha)^{61}Co$.

Figure 3 $\sigma_{e,2n}(E_o)$ for ^{63}Cu (circles) and the yield of electro plus photodisintegration (squares). The smooth curves are the best fit to the data and were obtained by combining the histogram shown in Fig. 5 with the El virtual photon spectrum and the DBM bremsstrahlung cross section in Eqs. (1) and (2).

Figure 4 $\sigma_{e,\alpha}(E_o)$ for ^{65}Cu (circles) and the yield of electro plus photodisintegration (squares). The smooth curves are the best fit to the data and were obtained by combining the El and E2 histograms of Fig. 7 with the virtual photon spectra and the DBM bremsstrahlung cross section in Eqs. (1) and (2). The triangles show the (e,α) cross section from ref. 6.

Figure 5 $^{63}Cu(\gamma,2n)$ cross section. The histogram is the result derived from this work and the points show the measurement of Fultz et al.[1] .

Figure 6 Ratio of measured to calculated (e,2n) cross section (circles) and measured to calculated yield of electro plus photodisintegration (triangles).

Figure 7 $^{65}Cu(\gamma,\alpha)$ cross sections. The El and E2 histograms are the results from this work. The points show the (γ,α) cross section from Ref. 6

Figure 8 Ratio of the (e,α) cross section from Ref. 6 and this work.

TABLE I

Target properties and separation energies

Target	^{63}Cu	^{65}Cu
Enrichment (%)	99.89	99.69
Thickness (mg/cm^2)	10.06±0.10	9.86±0.10
S(2n), MeV	19.7	17.8
S(α), MeV	5.8	6.76

TABLE II

Decay constants

Nucleus	$\lambda(min^{-1})$	Ref.
^{61}Co	$(6.95\pm0.29) \times 10^{-3}$	this work
	$(7.001\pm0.021) \times 10^{-3}$	8
^{61}Cu	$(3.56\pm0.18) \times 10^{-3}$	this work
	$(3.39\pm0.01) \times 10^{-3}$	9

TABLE III

(γ,α) strength for nuclei in the A=60 region. E1 sum: 60 NZ/A MeV.mb; E2 sum: 0.22 Z^2 $A^{-1/3}$ μb/MeV.

Nucleus	$\int_0^{30} \sigma_{\gamma,\alpha}(E)dE$ (MeV.mb)	Fraction of E1 sum	Fraction of E2 sum	Ref.
^{56}Fe	21 ± 3	2.1 ± 0.3	7 ± 1	2
^{58}Ni	43 ± 4	3.9 ± 0.4	21 ± 3	1
^{59}Co	17 ± 2	1.7 ± 0.2	5 ± 1	2
^{60}Ni	41 ± 4	3.5 ± 0.4	21 ± 5	1
^{62}Ni	17 ± 2	1.5 ± 0.2	8 ± 2	1
^{64}Zn	78 ± 16	6.9 ± 1.5	25 ± 3	2
^{65}Cu	10 ± 1	1.0 ± 0.1	3 ± 1	this work

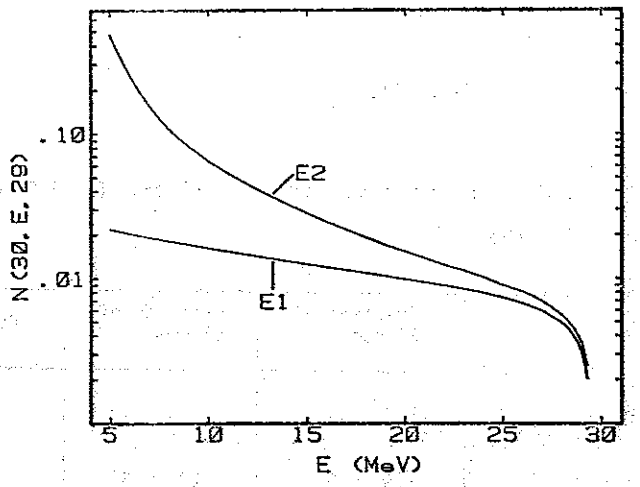

Fig. 1

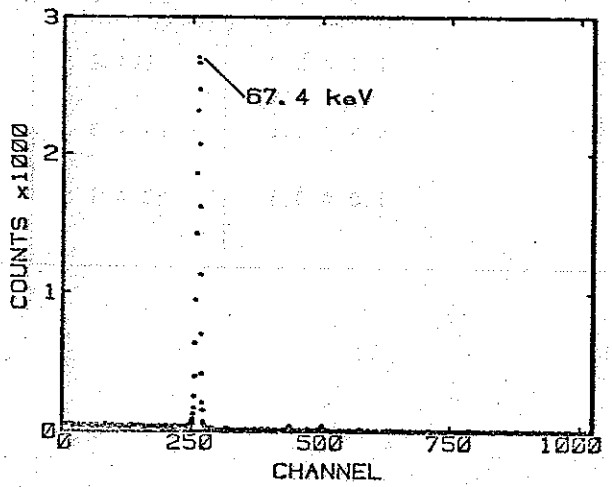

Fig. 2

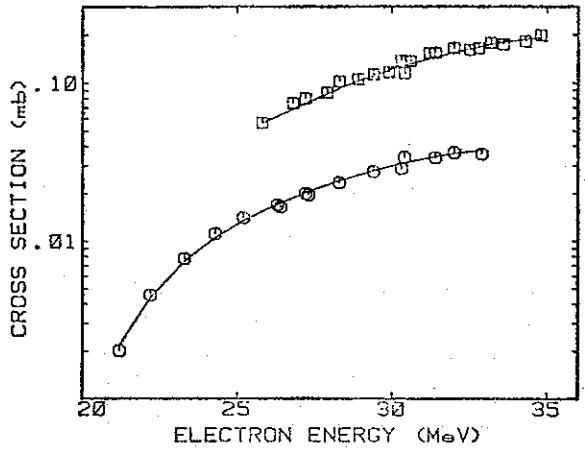

Fig. 3

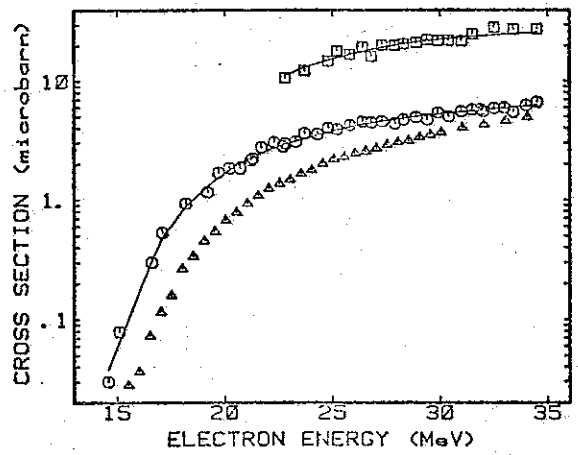

Fig. 4

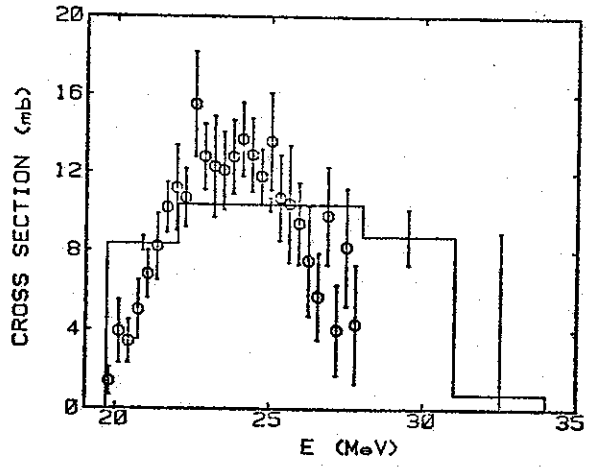

Fig. 5

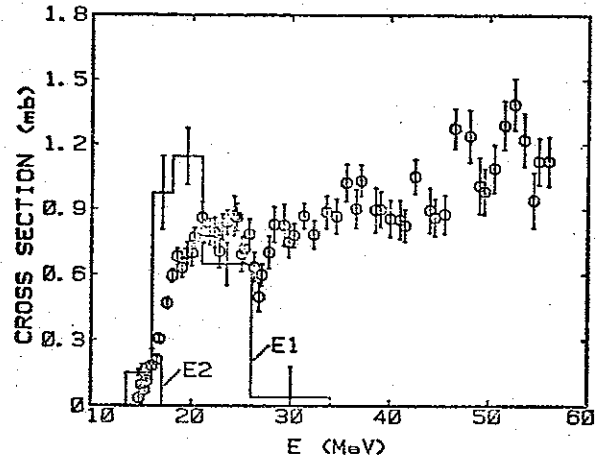

Fig. 7

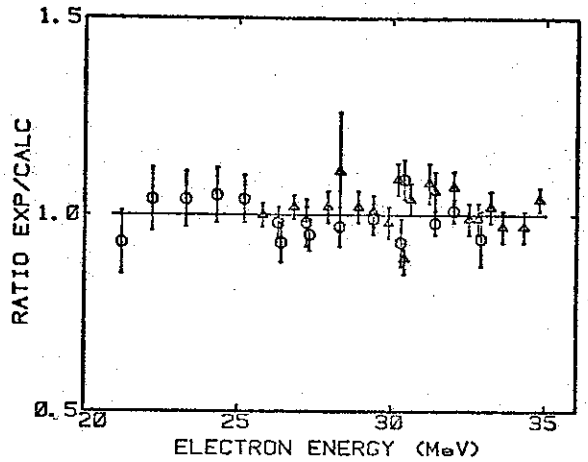

Fig. 6

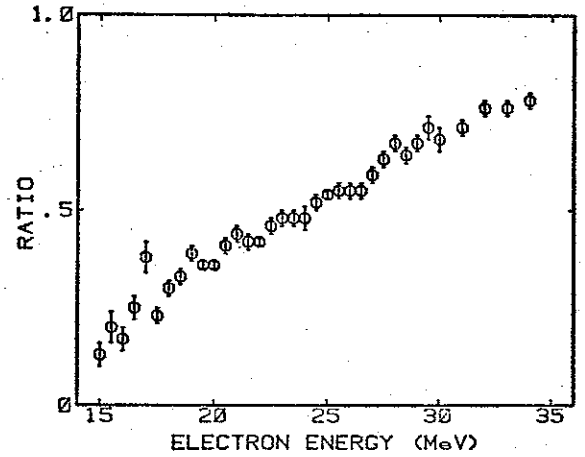

Fig. 8